Cell

Hedgehog Partial Agonism Drives Warburg-like Metabolism in Muscle and Brown Fat

Raffaele Teperino,[1,12] Sabine Amann,[2,12] Martina Bayer,[2,12] Sean L. McGee,[3] Andrea Loipetzberger,[4] Timothy Connor,[3] Carsten Jaeger,[5] Bernd Kammerer,[5] Lilli Winter,[6] Gerhard Wiche,[6] Kevin Dalgaard,[1] Madhan Selvaraj,[1] Michael Gaster,[7] Robert S. Lee-Young,[8] Mark A. Febbraio,[8] Claude Knauf,[9] Patrice D. Cani,[10] Fritz Aberger,[4] Josef M. Penninger,[11] J. Andrew Pospisilik,[1,*] and Harald Esterbauer[2,*]

[1]Max Planck Institute of Immunobiology and Epigenetics, Stuebeweg 51, D-79108 Freiburg, Germany
[2]Department of Laboratory Medicine, Medical University Vienna, Waehringer Guertel 18-20, A-1090 Vienna, Austria
[3]Metabolic Remodeling Laboratory, Metabolic Research Unit, School of Medicine, Deakin University, 75 Pigdons Road, Geelong, Victoria 3220, Australia
[4]Department of Molecular Biology, University of Salzburg, Hellbrunnerstrasse 34, A-5020 Salzburg, Austria
[5]Metabolomics Core, Center for Biological Systems Analysis (ZBSA), Habsburgerstrasse 49, D-79104 Freiburg, Germany
[6]Department of Biochemistry and Cell Biology, Max F. Perutz Laboratories, Dr. Bohr-Gasse 9, A-1030 Vienna, Austria
[7]Departments of Pathology and Endocrinology, Odense University Hospital, J.B. Winsløwsvej 25, DK-5000 Odense, Denmark
[8]Cellular and Molecular Metabolism Laboratory, Baker IDI Heart and Diabetes Institute, 75 Commercial Road, Melbourne, 3004, Australia
[9]INSERM U1048, Team 3, Institut de Medecine Moleculaire de Rangueil, Paul Sabatier University, Bat. L4, IFR150, CHU Rangueil, BP 84225, F-31432 Toulouse Cedex 4, France
[10]Université Catholique de Louvain, Louvain Drug Research Institute, Metabolism and Nutrition Research Group, Av. E. Mounier 73, B-1200 Brussels, Belgium
[11]Institute of Molecular Biotechnology of the Austrian Academy of Science, Dr. Bohrgasse 3, A-1030 Vienna, Austria
[12]These authors contributed equally to this work
*Correspondence: pospisilik@ie-freiburg.mpg.de (J.A.P.), harald.esterbauer@meduniwien.ac.at (H.E.)
http://dx.doi.org/10.1016/j.cell.2012.09.021

SUMMARY

Diabetes, obesity, and cancer affect upward of 15% of the world's population. Interestingly, all three diseases juxtapose dysregulated intracellular signaling with altered metabolic state. Exactly which genetic factors define stable metabolic set points in vivo remains poorly understood. Here, we show that hedgehog signaling rewires cellular metabolism. We identify a cilium-dependent Smo-Ca^{2+}-Ampk axis that triggers rapid Warburg-like metabolic reprogramming within minutes of activation and is required for proper metabolic selectivity and flexibility. We show that Smo modulators can uncouple the Smo-Ampk axis from canonical signaling and identify cyclopamine as one of a new class of "selective partial agonists," capable of concomitant inhibition of canonical and activation of noncanonical hedgehog signaling. Intriguingly, activation of the Smo-Ampk axis in vivo drives robust insulin-independent glucose uptake in muscle and brown adipose tissue. These data identify multiple noncanonical endpoints that are pivotal for rational design of hedgehog modulators and provide a new therapeutic avenue for obesity and diabetes.

INTRODUCTION

Hedgehog was initially described as a morphogen defining body patterning (Nüsslein-Volhard and Wieschaus, 1980). In mammals, ligand binding to the inhibitory cell surface receptor Patched (Ptch) permits Smoothened (Smo) translocation to the tip of the cilium and liberates zinc finger family transcription factors Gli1, Gli2, and Gli3 from proteasomal degradation and inhibitory tethering leading to activation of Gli target genes (Hui and Angers, 2011; Ingham et al., 2011; Riobo and Manning, 2007; Rohatgi and Scott, 2007; Ruiz i Altaba et al., 2007). Three highly homologous mammalian ligands exist for *Drosophila* hedgehog, namely Desert, Indian, and Sonic hedgehogs (Dhh, Ihh, and Shh, respectively). Whereas the majority of hedgehog-induced biological effects are thought to result from transcriptional regulation, several Gli-independent, noncanonical modules have also been reported (Riobo and Manning, 2007; Teglund and Toftgård, 2010). Shh, for instance, rapidly stimulates Src family kinases to spatially direct axonal outgrowth in vitro (Yam et al., 2009), and all three hedgehog ligands have been shown to promote cytoskeletal rearrangement via a Smo-G_i-RhoA axis in endothelial cells (Chinchilla et al., 2010). Furthermore, coupling of hedgehog to Rho small GTPases has been linked to the activation of fibroblast migration (Polizio et al., 2011). More recently, Shh has been shown to boost Ca^{2+} and IP_3 transients in spinal neurons through a G-protein- and Ca^{2+}-dependent pathway (Belgacem and Borodinsky, 2011).

Hedgehog activation impacts dozens of cellular processes, including stem cell renewal, lineage decision, cell-cycle regulation, migration, and mitogenic signaling (Hui and Angers, 2011; Ingham et al., 2011; Rohatgi and Scott, 2007; Ruiz i Altaba et al., 2007; Teglund and Toftgård, 2010). Accordingly, activating mutations in hedgehog pathway members have been causally implicated in a number of disparate cancers, including medulloblastoma, basal cell carcinoma, pancreatic cancers, and cancers of the intestinal tract (Ng and Curran, 2011; Teglund and Toftgård, 2010). Also, hedgehog signaling specifically blocks white, but not brown, adipogenesis (Pospisilik et al., 2010; Suh et al., 2006). This biological effect is sensitive to inflammatory state (Todoric et al., 2011) and represents one of the few known signaling nodes that are capable of differentially regulating brown versus white adipocyte differentiation (Lowe et al., 2011). All three factors—inflammation, adipocyte turnover, and adipose subtype distribution—show substantial imbalance in obesity and represent targets for therapeutic intervention (Lumeng and Saltiel, 2011; Whittle et al., 2011). Inhibitors of hedgehog signaling from at least seven pharmaceutical companies are currently in clinical trials (Ng and Curran, 2011). Intriguingly, despite their advanced development, a universal mechanism underlying hedgehog inhibitor efficacy is lacking. Specifically, potency of canonical hedgehog pathway inhibition does not match potency of inhibition of cancer growth (Yauch et al., 2008). One proposed mechanism to explain these anomalies has been indirect cancer modulation through paracrine or mesenchyme-tumor interaction (Chen et al., 2011; Chinchilla et al., 2010; Theunissen and de Sauvage, 2009; Yauch et al., 2008).

In the current study, we show that hedgehog stimulates metabolic reprogramming toward a Warburg-like glycolytic state. The effect, mediated by a rapid noncanonical Smo-Ca^{2+}-Ampk signaling arm effects robust glucose uptake in vivo in the mouse and in human myocytes and surprisingly is also induced by several canonical hedgehog inhibitors. The results provide critical insights into the substantial hedgehog inhibitor side effects in humans and into the complexity of hedgehog signaling itself, and they raise new therapeutic strategies for obesity and type-1 diabetes.

RESULTS

Hedgehog Reprograms Energy Metabolism

Hedgehog signaling regulates multiple cellular processes, including two with finely tuned metabolic programs, namely cancer and adipose tissue development. We asked whether hedgehog might determine metabolic state. We chose 3T3-L1 adipocytes as a model because they exhibit some of the best characterized metabolic regulatory circuits and they respond fully to hedgehog (Pospisilik et al., 2010). Intriguingly, stimulation of mature 3T3-L1 adipocytes with *smoothened agonist* (SAG) (Chen et al., 2002b), a small molecule activator of Smo, led to acidification of culture media within 24 hr (Figure 1A). Quantitation revealed increased extracellular acidification (ECAR) and reduced oxygen consumption (OCR) rates upon SAG stimulation (Figure 1B), findings that are consistent with reduced glucose and increased lactate levels in the culture medium (Figure 1C). Further, levels of the oxidized redox equivalents NAD^+ and $NADP^+$ (Figure 1D) were elevated, indicating substrate rerouting away from energy production. Importantly, reduced forms of the redox equivalents NADH and NADPH remained unchanged, as did ATP levels, yielding an overall increase in redox ratios (Figure 1E and Figures S1A and S1B available online). This metabolic reset was reminiscent in many ways to the Warburg effect observed in cancer and to the metabolic rearrangements that characterize stem cell renewal and immune cell activation (Hsu and Sabatini, 2008; Shi et al., 2011; Vander Heiden et al., 2009). Importantly, no evidence of proliferation was found in these terminally differentiated, growth-arrested cells. Pathway stimulation using the endogenous ligand Shh recapitulated all key aspects of the metabolic phenotype (Figures 1F–1H and S1C), and, whereas wild-type primary mouse embryonic fibroblasts (MEFs) exhibited significant SAG-stimulated metabolic shifts, $Smo^{-/-}$ MEFs (Varjosalo et al., 2006) showed none (Figures 1I–1K), thus ruling out potential chemical artifacts. Importantly, these findings were recapitulated in the 3T3-L1 system upon Smo knockdown (Figures S1D–S1F). Thus, hedgehog signaling reprograms adipocyte metabolism toward aerobic glycolysis.

Hedgehog Triggers Rapid Metabolic Rewiring via Ampk

Next, we performed a time course of glucose removal from and lactate accumulation into 3T3-L1 culture supernatants. Surprisingly, marked glucose removal and lactate generation were observed within minutes of SAG addition (Figures 2A and 2B), a finding completely inconsistent with transcriptionally driven canonical hedgehog signaling (Figure S2A). To understand how Smo activation could lead to such rapid metabolic reprogramming, we performed a phosphoproteomic survey of the acute hedgehog signaling response. Two-dimensional gel electrophoresis was used to resolve phospho-enriched lysates from differentiated 3T3-L1 adipocytes treated for 10 min with or without SAG (Figure 2C). Of the 632 spots that were consistently detected in three independent experiments, 55 spots comprising 39 specific phosphoproteins showed reproducible differential regulation > 1.5-fold (Table S1). This data set presents an unbiased snapshot of rapid noncanonical hedgehog signaling and identifies numerous downstream signaling activities not previously associated with hedgehog. Intriguingly, in a KEGG pathway analysis, all significantly enriched gene sets except one constituted compartments of primary energy metabolism, including *glucose*, *ketone body*, *fatty acid*, *pyruvate*, and *ketogenic amino acid metabolism*, as well as the *TCA cycle* (Figure 2D and Table S2). Numerous key regulators of glucose and energy metabolism were identified, including acetyl-CoA acetyltransferase (Acat1), glyceraldehyde-3-phosphate dehydrogenase (Gapdh), transaldolase 1 (Taldo1), hormone-sensitive lipase (Lipe), phosphoglycerate mutase (Pgam1), glycogen synthase (Gys), and pyruvate dehydrogenase alpha 1 (Pdha1) (Figure 2E), indicating that a complex metabolic signaling network exists that is rapidly accessible to Smoothened. Of interest, the only nonmetabolic pathway enriched in our analysis was the *proteasome*, a well-known and integral component of canonical hedgehog signaling (Hui and Angers, 2011; Teglund and Toftgård, 2010). Thus, hedgehog rapidly signals to the machinery of primary energy metabolism.

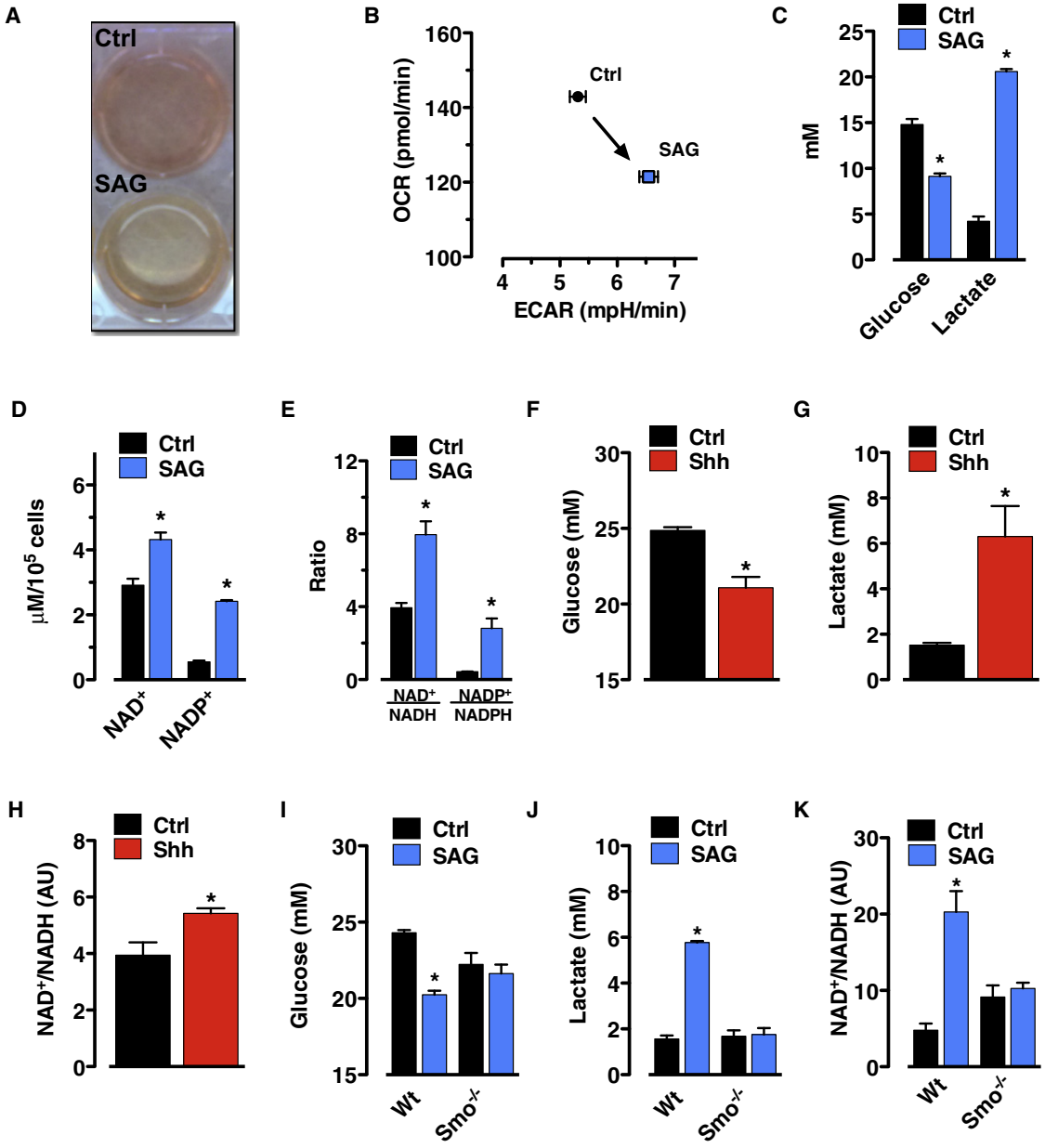

Figure 1. Hedgehog Reprograms Adipocyte Metabolism

(A–E) Differentiated 3T3-L1 adipocytes treated with SAG (200 nM) acidify growth medium (A); display reduced O_2 consumption (OCR) and increased extracellular acidification (ECAR) (B); utilize more glucose and produce more lactate (C); and show increased NAD^+, $NADP^+$ (D) and their ratios within 24 hr of treatment (E). (F–H) Similarly, treatment with Sonic hedgehog (Shh) increased glucose consumption (F), lactate production (G), and NAD^+/NADH ratio (H).

(I–K) Unlike wild-type (WT) MEFs, *Smo*$^{-/-}$ MEFs are not responsive to SAG in terms of glucose consumption (I), lactate production (J), or change in NAD^+/NADH ratio (K).

Results are mean ± SEM. n = 4–6 independent experiments. *$p < 0.05$ compared to vehicle-treated samples. See also Figure S1.

To further characterize the hedgehog-driven metabolic phenotype, we performed western blot time course analysis of Pdha1, AMP-activated protein kinase (Ampk), and pyruvate kinase M1/M2 (Pkm2) phosphorylation events. All three proteins have key roles in deciding glycolytic substrate fate and anabolic-to-catabolic transitions and have been implicated in the regulation of the Warburg effect and cancer cell growth (Hitosugi et al., 2009; Jeon et al., 2012; Vander Heiden et al., 2009). Intriguingly, robust phosphorylation signals were observed from all three proteins within 2 min of either SAG (Figure 2F) or Shh (Figure S2B), modifications that are consistent with enhanced glycolysis.

Could Ampk, Pdha1, and Pkm2 be responsible for the observed metabolic phenotype? shRNA knockdown of Ampk

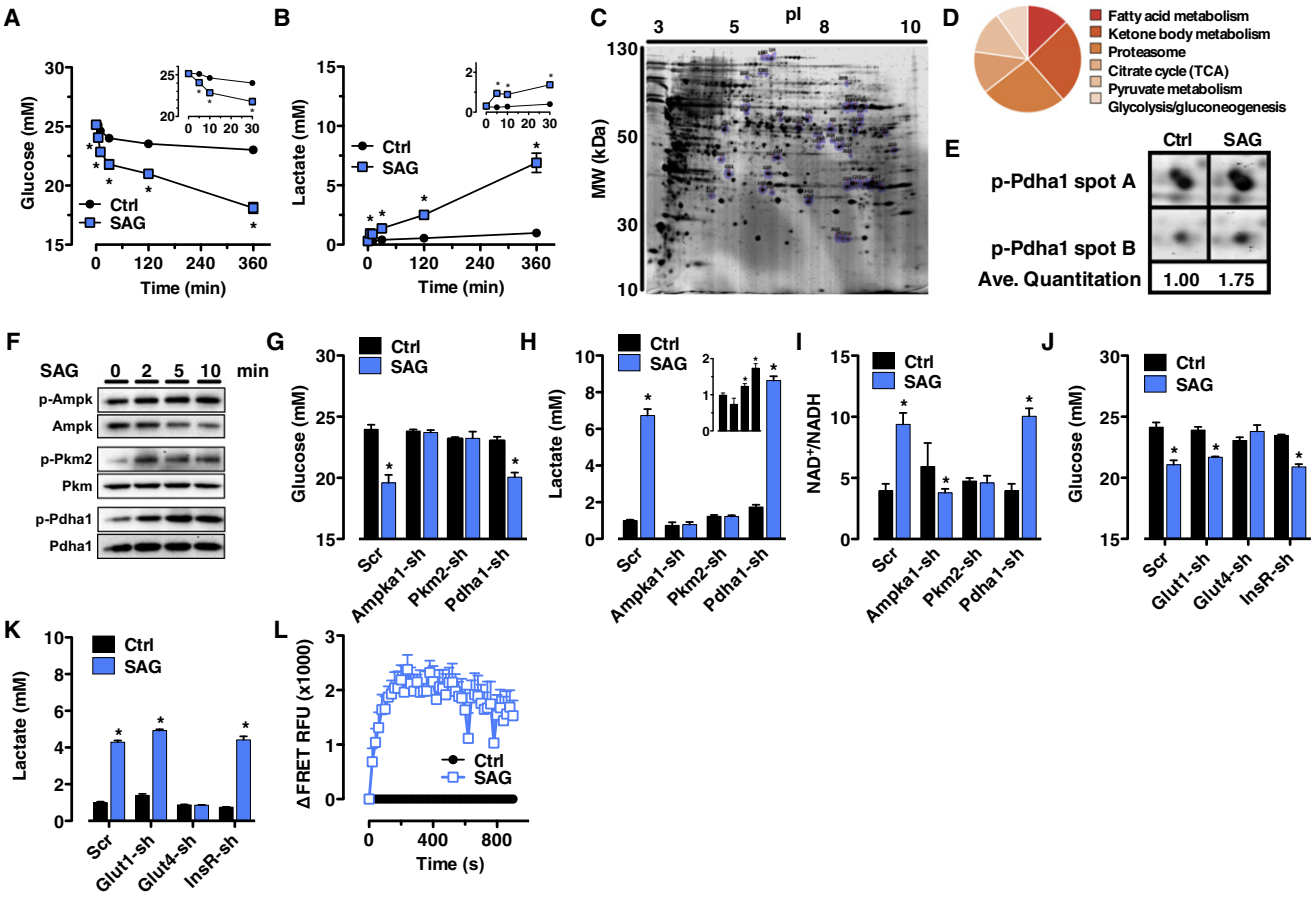

Figure 2. Hedgehog Triggers Rapid Metabolic Rewiring via Ampk

(A and B) SAG-treated 3T3-L1 adipocytes increase glucose consumption (A) and lactate production (B) within minutes.

(C) Phospho-2D-gel highlighting spots changed within 10 min of SAG addition.

(D) KEGG pathway analysis of differentially regulated phosphoproteins.

(E) Two significantly phosphorylated spots corresponding to Pdha1.

(F) Western blot time course of SAG-induced protein phosphorylation in 3T3-L1 adipocytes.

(G–K) Ampk and Pkm2 knockdown abrogates SAG-induced glucose disposal (G), lactate production (H), and elevation in NAD^+/NADH ratio (I). Glut4 knockdown blunts SAG-induced glucose uptake (J) and lactate production (K).

(L) A plasmid-encoded FRET based assay in HEK293 cells shows rapid induction of AMPK activity upon SAG treatment.

Results are mean ± SEM. n = 4–6 independent experiments. *p < 0.05 compared to vehicle-treated samples (A and B) or scrambled shRNA-transfected cells (G–K). See also Figure S2.

in 3T3-L1 adipocytes (Figure S2C) completely abolished SAG-stimulated disruption of redox balance, extracellular glucose/lactate levels, and OCR/ECAR flux levels (Figures 2G, 2H, and S2D). Similarly, preincubation of cells with compound C, an inhibitor of Ampk activity, abrogated detectable metabolic rewiring effects following SAG stimulation in both fully differentiated 3T3-L1 adipocytes (Figures S2D–S2F) and MEFs (Figures S2G and S2H). Importantly, OCR/ECAR measures confirmed that neither Ampk knockdown nor Ampk inhibition alone reduced metabolic rate. Knockdown of Pdha1 on the other hand (Figure S2I), a genetic mimic of its phosphorylation-mediated inhibition, showed no apparent effect on SAG-induced glucose uptake (Figure 2G) but substantially enhanced cellular lactate release (Figure 2H) and redox rebalancing (Figure 2I). Disruption of Pkm2 (Figure S2I), interestingly, blunted any sign of a SAG-inducible glucose/lactate response and increased basal lactate accumulation (Figures 2G and 2H). Collectively, these results suggest that Ampk and Pkm2 mediate SAG-induced glucose uptake, whereas Pkm2 and Pdha1 focus substrate flux toward lactate. In keeping with a largely Ampk-driven process, SAG-induced glucose uptake was Glut4 dependent, but neither Glut1 dependent nor insulin receptor dependent (Figures 2J, 2K, and S2I). Thus, Smo activation drives Ampk/Pkm2/Pdha1-dependent metabolic rewiring.

To better define the kinetics of the noncanonical response, we used AMPKAR, a Foerster resonance energy transfer (FRET) probe for AMPK activity (Tsou et al., 2011). Because transfection and FRET signal detection in mature adipocytes is poor, we used HEK293 cells, which have previously been used for high-throughput hedgehog screening (Roudaut et al., 2011).

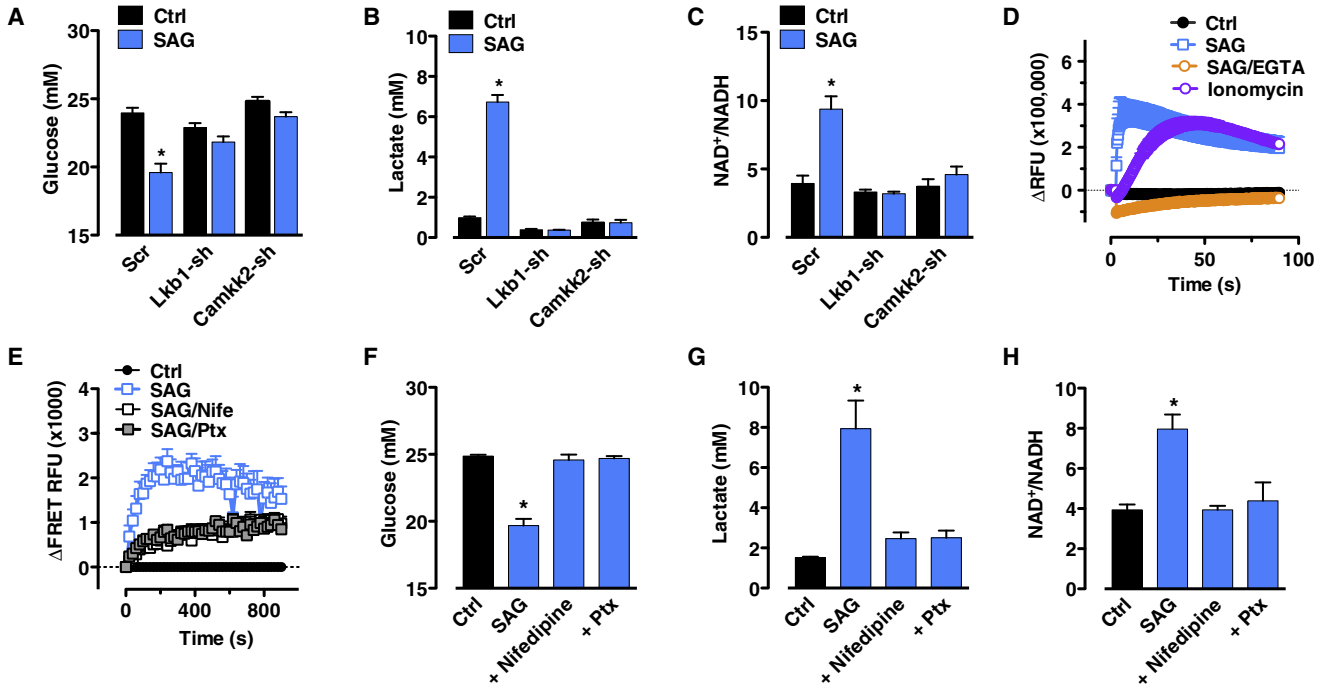

Figure 3. A Smo-Camkk2-Ampk Axis

(A–C) Lkb1 and Camkk2 knockdown abrogates SAG-induced glucose disposal (A), lactate production (B), and NAD^+/NADH elevation (C) in 3T3-L1 adipocytes.

(D) SAG-treated adipocytes show a rapid and robust calcium response completely blunted by the extracellular calcium chelator EGTA (1 μM).

(E) SAG-induced AMPK activity in AMPK-AR reporter expressing HEK293 cells is inhibited by both Nifedipine and Ptx.

(F–H) Nifedipine (20 μM) or Ptx (100 ng/ml) treated 3T3-L1 adipocytes are refractory to SAG-induced glucose disposal (F), lactate production (G), and NAD^+/NADH elevation (H).

Results are mean ± SEM. n = 4–6 independent experiments. *$p < 0.05$ compared to scrambled shRNA-transfected cells (A–C) or vehicle-treated samples (F–H). See also Figure S3.

Intriguingly, addition of SAG to AMPKAR-expressing HEK293 cells revealed rapid and sustained AMPK-FRET signals detectable within 20 s of SAG addition (Figure 2L). Thus, hedgehog stimulates rapid activation of AMPK in human and mouse cells and across disparate cell types.

A Smo-Camkk2/Lkb1-Ampk Axis

Though predominantly studied as an activator of Gli-dependent transcriptional regulation over hours or days, Smo is a class F G-protein-coupled receptor (Ogden et al., 2008; Polizio et al., 2011), a class of proteins that effect rapid G-protein-coupled second messenger signals. Ampk is principally stimulated by increased AMP/ATP ratio and by the upstream kinases serine/threonine-protein kinase 11 (Lkb1) and calcium/calmodulin-dependent protein kinase kinase 2 (Camkk2) (Cantó and Auwerx, 2011; Hardie, 2011). Using GC/MS, no marked dysregulation in AMP, ADP, or ATP was observed (Figure S3A), indicating normal AMP-to-ATP balance. Knockdown of either Lkb1 or Camkk2 (Figures S3B–S3D), however, resulted in near-complete abrogation of SAG-stimulated metabolic sequelae (Figures 3A–3C and S3E), suggesting that both proteins couple Smo to Ampk. Importantly, though resistant to Smo-dependent metabolic rewiring, both Lkb1 and Camkk2 knockdown adipocytes responded fully to AICAR (Figures S3F–S3H), indicating that Ampk signaling in these cells remained intact.

In line with a key role for Camkk2, SAG stimulation of adipocytes preloaded with the Ca^{2+}-sensitive fluorophore Fluoforte-AM revealed a Ca^{2+} response that is more rapid and intense than a standard 1 μM ionomycin stimulation (Figure 3D). The same was true for the endogenous ligand Shh (Figure S3I). Administration of the extracellular calcium chelator EGTA under the same conditions completely abrogated SAG- and Shh-induced responses, indicating that Smo activation promotes opening of plasma membrane Ca^{2+} channels rather than mobilizing of intracellular stores (Figures 3D and S3I). Importantly, the L-type calcium channel blocker Nifedipine markedly blunted both Ampk activity (Figures 3E, S3J, and S3K) and the observed metabolic phenotype (Figures 3F–3H). Moreover, Pertussis toxin (Ptx), a potent inhibitor of receptor-to-$G\alpha_i$ G protein coupling, blunted Ampk activation and metabolic rerouting (Figures 3E–3H). Thus, a rapid Ca^{2+}- and $G\alpha_i$-dependent noncanonical Smo-Ampk signaling axis rewires metabolism.

Noncanonical Rewiring of Metabolism Is Primary Cilium Dependent

Canonical hedgehog signaling requires Smo translocation to the primary cilium (Corbit et al., 2005; Rohatgi et al., 2007, 2009; Wang et al., 2009). We used cilia-deficient *Ift88*$^{-/-}$ and *Kif3a*$^{-/-}$ MEFs and their respective control cell lines to probe the cilia dependence of our system. Intraflagellar transport protein 88

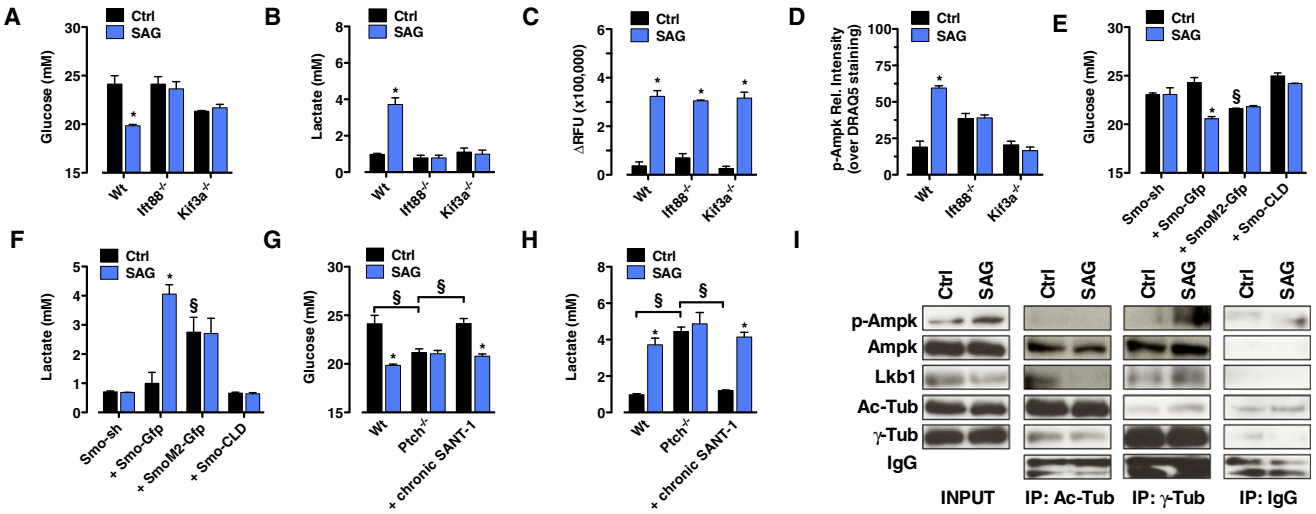

Figure 4. Noncanonical Rewiring of Metabolism Is Primary Cilium Dependent

(A–D) MEFs derived from either Ift88 or Kif3a knockout mice show no SAG-induced glucose disposal (A), lactate production (B), or Ampk activation (D) despite an intact Ca^{2+} response (C).

(E and F) Smo knockdown abrogates SAG-induced glucose disposal (E) and lactate production (F) in 3T3-L1 adipocytes, effects that are rescued by the reintroduction of wild-type Smo, but not SmoM2 and Smo-CLD mutants.

(G and H) MEFs derived from *Ptch*$^{-/-}$ mice show increased basal glucose disposal (G) and lactate production (H) with no further SAG response. Responsiveness is restored by chronic treatment with 100 nM SANT-1.

(I) Coimmunoprecipitation analysis of the Smo-Lkb1-Ampk axis.

Results are mean ± SEM. n = 4–6 independent experiments. *p < 0.05 compared to vehicle-treated samples (A–H). §p < 0.05 compared to Smo-KD (E and F) or *Ptch*$^{-/-}$ cells (G and H). See also Figure S4.

(Ift88) and kinesin family member 3A (Kif3a) are required for proper ciliogenesis, and their loss results in lack of canonical hedgehog signaling competency and of a functional primary cilium. Strikingly, whereas control MEFs showed full noncanonical responses to SAG induction, glucose uptake and lactate production were severely blunted in the mutant lines (Figures 4A and 4B). Importantly, both mutant cell lines exhibited a significant Ca^{2+} response to SAG (Figure 4C), but neither exhibited any sign of Ampk activation by in-cell western blot (Figures 4D and S4A), indicating that the cilium is necessary to couple Smo-induction to Ampk activity. Of note, both lines mounted significant metabolic responses to AICAR, indicating uncompromised Ampk and downstream signaling (Figures S4B–S4D). Thus, the Smo-Ampk response is dependent on the primary cilium.

To corroborate these findings in the adipocyte system, we tested the ability of several Smo variants to rescue the stable loss of function in our Smo knockdown 3T3-L1 cells (Figures 4E and 4F). As expected, wild-type Smo-GFP rescued noncanonical signaling competency in the mature knockdown adipocytes. However, transfection with a cilia localization-deficient Smo mutant (Smo-*CLD*) was completely incapable of restoring responsiveness (Figures 4E, 4F, and S4E). This variant harbors a mutation in two amino acids that are necessary for Smo ciliary translocation (Corbit et al., 2005). Surprisingly, reconstitution with the constitutively active SmoM2 mutant also failed to rescue metabolic responsiveness to SAG (Figures 4E, 4F and S4E). Of note though, SmoM2-reconstituted 3T3-L1 cells did exhibit a moderate increase in glucose uptake and lactate accumulation in the basal state. Knowing that canonical activation requires a second step of Smo translocation from the base to the tip of the cilium and that SmoM2 accumulates toward the tip (Han et al., 2008), these findings suggested that the base of the cilium could be critical in linking Smo induction to Ampk activation. This interpretation is consistent with the observations that *Ptch*$^{-/-}$ MEFs (constitutively active canonical signaling) exhibit metabolic rewiring in the basal state and show a lack of responsiveness to SAG that can be reversed by long-term treatment with the Ampk blocker compound C. Also, both the basal hyperactivation and the lack-of-responsiveness phenotypes can be rescued by long-term preincubation with SANT-1 (Figures 4G and 4H), which blocks Smo translocation to the cilium base.

Boehlke et al. recently reported a cilium-based system in kidney epithelial cells coupling mechanical sensation of fluid flow to cell size regulation via basal-body-restricted Lkb1 and Ampk (Boehlke et al., 2010). We used coimmunoprecipitation to test whether an analogous system might be at play here. Importantly, Lkb1 and Ampk enriched in the γ-tubulin immunoprecipitation of mature 3T3-L1 cells (Figure 4I, third column), indicating the presence of both proteins at the basal body. Similarly, we observed Lkb1 and Ampk signals pulled down by acetylated α-tubulin (Figure 4I, second column), indicating their presence in the cilium. Critically, upon SAG activation, we observed: (1) robust enrichment of P-Ampk with γ-tubulin pull-down, identifying a spatial node for noncanonical signaling at the basal body (Figure 4I, third column, top), (2) depletion of Lkb1 from the acetylated α-tubulin compartment, and (3) apparent accumulation of Lkb1 at γ-tubulin. Thus, noncanonical Smo signaling to Ampk appears compartmentalized at the basal body.

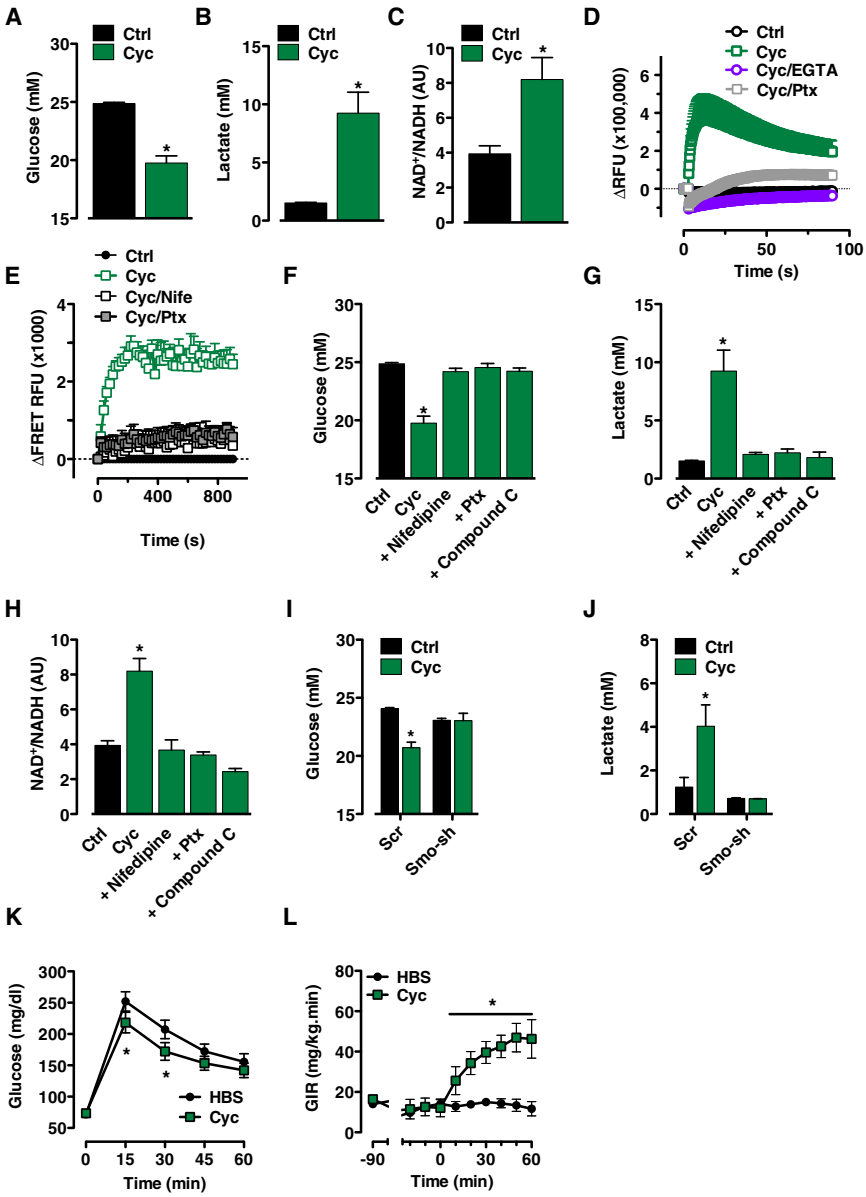

Figure 5. Smo-Ampk-Selective Partial Agonism Stimulates Glucose Uptake In Vivo

(A–C) Cyclopamine (100 nM) induces metabolic reprogramming in differentiated 3T3-L1 adipocytes increasing glucose consumption (A), lactate production (B), and NAD^+/NADH (C).

(D) Cyclopamine elicits a rapid EGTA-sensitive Ca^{2+} response.

(E) AMPK-AR-expressing HEK293 cells show rapid induction of AMPK activity upon cyclopamine treatment, an effect that is blunted by both Nifedipine and Ptx.

(F–H) Cyclopamine-induced glucose consumption (F), lactate production (G), and elevation of NAD^+/NADH (H) are also abrogated by Nifedipine, Ptx, and compound C.

(I and J) Smo knockdown 3T3-L1 adipocytes show no sign of cyclopamine-induced glucose disposal (I) and lactate production (J).

(K) C57BL/6J mice display improved glucose tolerance (n = 12) when pretreated with cyclopamine (10 mg/kg, i.p.; n = 12) relative to vehicle alone (HBS).

(L) Increased glucose infusion rate (GIR) during glycemic-insulinemic clamps (n = 6–10).

Results represent mean ± SEM. n = 4–6 independent experiments in vitro. *p < 0.05 compared to vehicle-treated samples. See also Figure S5.

Selective Partial Agonism of Metabolic Rewiring In Vitro and In Vivo

Numerous inhibitors of canonical hedgehog signaling are in clinical trials for their anticancer potential (Ng and Curran, 2011). To tease apart the relative contributions of canonical Gli-dependent and noncanonical Ampk-dependent signaling, we began to test well-characterized hedgehog antagonists for their potential to block the identified rapid metabolic response. Surprisingly, when adding the classic hedgehog antagonist cyclopamine (Chen et al., 2002a), initially as a negative control, we observed rapid and robust metabolic reprogramming analogous to that induced by SAG (Figures 5A–5C). These effects were observed at 100 nM, where cyclopamine binds efficiently to Smo but is incapable of displacing SAG from their shared binding site to block canonical signaling (Chen et al., 2002a, 2002b). Importantly, cyclopamine is known to cause Smo translocation to the basal body of the cilium at these concentrations. Further, cyclopamine induced rapid and robust Ca^{2+} and AMPKAR responses sensitive to both extracellular EGTA and Ptx (Figures 5D and 5E), suggesting that SAG and cyclopamine induce a common noncanonical signal. Critically, cyclopamine-dependent glucose uptake, lactate production, and redox rebalancing were also all efficiently counteracted by addition of Nifedipine, Ptx, or the Ampk inhibitor compound C (Figures 5F–5H) and via knockdown of Smo in the 3T3-L1 system (Figures 5I and 5J). Thus, (1) Smo modulators can activate noncanonical signaling independently of the canonical arm, (2) canonical and noncanonical signaling arms can be uncoupled via the SAG/cyclopamine binding site of Smo, and (3) cyclopamine is a potent selective partial agonist of the noncanonical pathway.

Of chief importance, these findings provided us with a tool to probe the relevance of the noncanonical axis in vivo. To test whether Smo-selective partial agonism could boost metabolism in vivo, we performed oral glucose tolerance tests (OGTT) on wild-type C57BL/6J mice in the presence or absence of acute cyclopamine pretreatment. Remarkably, mice receiving 10 mg/kg cyclopamine 15 min prior to testing displayed a moderate but significant improvement in glucose tolerance (Figure 5K). Of note, neither basal- nor glucose-stimulated insulin secretion appeared affected by the pretreatment (Figure S5A). Because

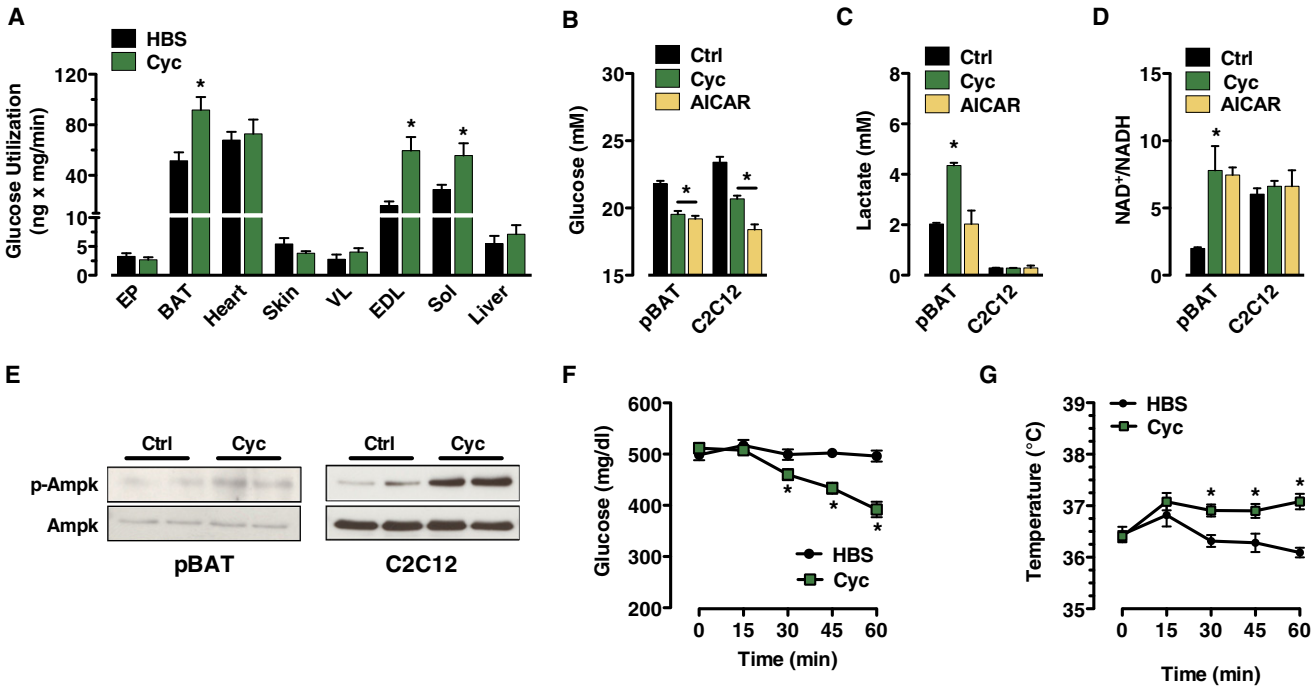

Figure 6. Insulin-Independent Glucose Uptake in Muscle and Brown Fat

(A) Glucose tracers revealed that cyclopamine enhances glucose uptake in BAT, EDL, and Soleus muscles (EP, epididymal adipose; BAT, brown adipose tissue; VL, vas lateralis; EDL, extensor digitorum longus; Sol, soleus).

(B–D) Whereas C2C12 myotubes exhibit only increased glucose disposal, primary brown adipocytes (pBAT) show increased glucose consumption (B), lactate production (C), and elevation of NAD^+/NADH (D) upon cyclopamine treatment. The chemical Ampk agonist AICAR (0.5 mM) only partially recapitulates the phenotypes.

(E) Western blot of cyclopamine-induced Ampk phosphorylation in pBAT and C2C12 myotubes.

(F and G) Cyclopamine treatment (10 mg/kg) induces glucose clearance and elevation in body temperature (n = 6–26) in insulin-deficient STZ-treated C57BL/6J mice.

Results are mean ± SEM. n = 4–6 independent experiments. *$p < 0.05$ compared to vehicle-treated samples. See also Figure S6.

insulin is known to counteract Ampk activity, we reasoned that an acute insulin response might be masking the full potential of the response. We therefore examined the response in hyperglycemic-insulinemic clamps exploiting continuous somatostatin infusion to suppress acute insulin responses. Impressively, under these conditions, cyclopamine infusion elicited robust glucose uptake (glucose infusion rate) within 10–20 min of stimulation (Figure 5L). Thus, Smo-selective partial agonism induces metabolic rewiring and acute glucose uptake in vivo.

Selective Partial Agonism Specifically Activates Muscle and Brown Fat

In addition, the clamp studies were designed to trace tissue-specific glucose uptake via introduction of a nonmetabolizable 2-deoxyglucose radiolabel. Intriguingly, rather than the anticipated white adipose tissue (WAT) glucose uptake, brown adipose tissue (BAT) and muscles of multiple fiber types (extensor digitorum longus, EDL, glycolytic; and soleus, Sol, oxidative) exhibited the dominant cyclopamine-induced glucose uptake responses in vivo (Figure 6A). To explore the cell autonomy of this surprising finding, we stimulated C2C12 myotubes and differentiated primary brown adipocytes (pBAT) with cyclopamine and measured glucose, lactate, and NAD^+/NADH endpoints as before. In keeping with the clamp results, both C2C12 and pBAT cells exhibited robust glucose uptake within 10 min of cyclopamine stimulation (Figure 6B). Brown adipocytes produced significant increases in lactate and NAD^+/NADH, whereas the myotubes, whose 10-fold lower lactate release rates suggest very high oxidative capacity, resisted both downstream metabolic sequelae (Figures 6C and 6D). These findings suggest that the exact metabolic end state resulting from Smo stimulation depends on the machinery of the tissue type in question. Importantly, we observed prominent P-Ampk responses to cyclopamine in both cell models (Figure 6E). Equally important, all key endpoints, including in vivo glycemic-insulinemic clamps, were recapitulated for SAG (Figure S6), corroborating the selectivity of cyclopamine-induced metabolic rewiring. Thus, selective partial agonism of the Smo-Ampk axis stimulates muscle and brown fat glucose uptake in mice.

These findings, observed under somatostatin infused conditions, raised the intriguing question of whether the system might be effective even in the absence of insulin. To test this hypothesis, we treated mice with high-dose streptozotocin (STZ) to selectively neutralize insulin secretory capacity and generate a type-1-diabetes-like state. Remarkably, despite a complete lack of circulating insulin, STZ-treated mice showed significant

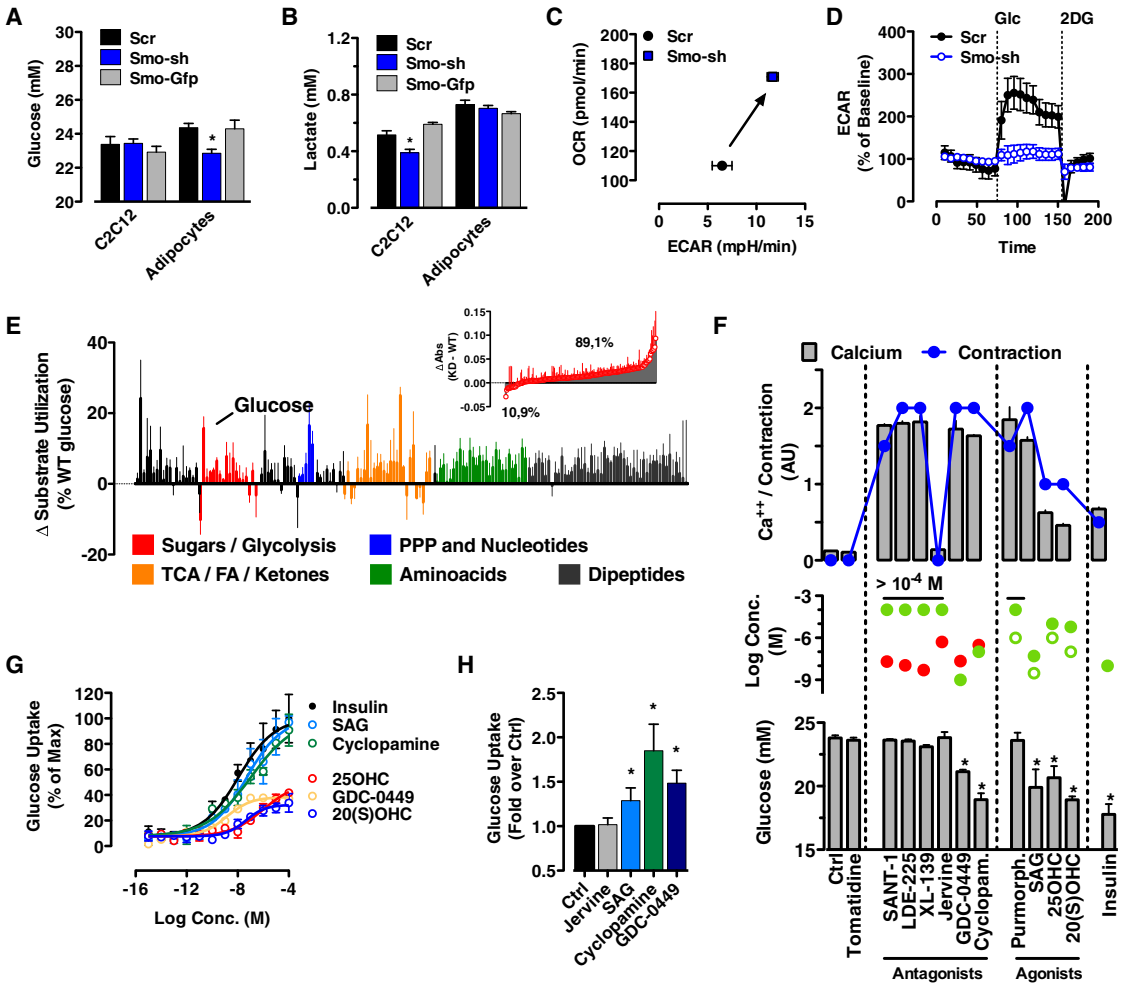

Figure 7. Smo Controls Metabolic Flexibility and Skeletal Muscle Contraction

(A and B) Smo knockdown increases basal glucose consumption in adipocytes (A) and decreases lactate production in C2C12 cells (B). Both effects are rescued by the reintroduction of wild-type Smo (A and B).

(C and D) Smo knockdown 3T3-L1 adipocytes exhibit increased metabolic rate (C) and complete lack of glycolytic flexibility upon glucose exposure (D).

(E) Smo knockdown adipocytes show increased metabolism of a broad range of carbon substrates.

(F) Assessment of a panel of Smo modulators revealed tight correlation between induction of a Ca^{2+} response and contraction and largely uncoupled canonical (red circles = IC_{50}; green open circles = EC_{50} Gli induction in Shh-Light2 cells) and noncanonical (green solid circles = EC_{50} glucose uptake) responses.

(G) Dose-response curves for all compounds inducing glucose uptake.

(H) SAG, cyclopamine, and GDC-0449 induce glucose disposal in primary human myocytes.

Results are mean ± SEM. n = 4–6 independent experiments in vitro. *p < 0.05 compared to vehicle-treated samples. See also Figure S7.

and robust glucose clearance within ~30 min of cyclopamine injection (Figure 6F). Further, in direct support of an endogenous glucose fate including brown adipose tissue, cyclopamine increased core body temperature ~1.0°C in the same mice over a 1 hr period (Figure 6G), suggesting that selective partial agonism of the Smo-Ampk axis activates thermogenesis in vivo. Thus, Smo-selective partial agonism induces insulin-independent and tissue-selective metabolic rewiring in vivo.

Smo Determines Metabolic Tone, Specificity, and Flexibility

A number of studies indicate that Smo itself may have endogenous ligands, including two oxysterols 20(s)-OHC and 25-OHC (Corcoran and Scott, 2006; Nachtergaele et al., 2012). Given the potent gluco-regulatory effects of SAG and cyclopamine, we revisited our in vitro system to ask whether endogenous Smo signaling might regulate metabolism. Indeed, Smo knockdown reduced the anaerobic-to-aerobic ratio (lactate generation/glucose uptake) in both 3T3-L1 and C2C12 cells, manifest as either an increase in glucose uptake (3T3-L1) or a reduction in lactate generation (C2C12) (Figures 7A and 7B). Thus, Smo appears to modulate metabolic tone independently of exogenous ligand stimulation.

Because Smo knockdown myocytes exhibited significant hypercontractility to even minor perturbations, we moved forward with Smo knockdown 3T3-L1 cells. Intriguingly, despite a high

metabolic rate, Smo knockdown cells were incapable of mounting a substantial switch to glucose utilization when shifted from no-glucose to high-glucose medium, responding with a 5-fold smaller OCR burst than control cells (Figures 7C, 7D, and S7A). Probing further, we used a panel of ~180 different carbon and nitrogen sources to fingerprint Smo knockdown cells metabolically. The test, performed in fuel-depleted medium, measures substrate utilization for a spectrum of fuel sources one substrate at a time. Intriguingly, Smo knockdown 3T3-L1 adipocytes exhibited increased fuel utilization for the majority of substrates tested, including a remarkable 29 substrates completely unprocessed in control adipocytes (Figure 7E). Removal of Smo appeared to short-circuit cell type restriction of fuel use, leaving cells able to metabolize a much wider substrate repertoire. Thus, Smo regulates metabolic flux, flexibility, and substrate specificity.

Noncanonical Signaling, Metabolism, and Side Effects

This year, the FDA approved the first hedgehog inhibitor, Vismodegib (GDC-0449), for cancer therapy use in humans. Clinical data are currently available for five hedgehog antagonists: GDC-0449, LDE-225, XL-139, IPI-926, and PF-0449913 (Li et al., 2012; Lin and Matsui, 2012; Low and de Sauvage, 2010; Von Hoff et al., 2009). Unfortunately, the first reports indicate side effects so severe that dropout rates have exceeded a discouraging 50% (Sekulic et al., 2012; Tang et al., 2012). Intriguingly, the physiological effects of our key noncanonical endpoints are highly consistent with the two major reported side effects: weight loss (Ampk; catabolism) and muscle cramping (Ca^{2+} influx). We probed our system to gain insight into whether noncanonical Smo signaling might be responsible for the side effect in humans. Intriguingly, initial testing revealed that all compounds except jervine induced contraction in myocytes (Figure 7F). Because contraction itself induces Ca^{2+} and Ampk-dependent glucose uptake, this finding precluded use of myocytes for quantitative determination of the noncanonical arm. We therefore interrogated the canonical antagonists cyclopamine, jervine, SANT-1, GDC-0449, LDE-225, and XL-139 and agonists purmorphamine, SAG and the oxysterols 20(s)-OHC and 25-OHC for their noncanonical and canonical potencies in mature 3T3-L1 adipocytes and Shh-Light2 cells (Figures 7F and 7G). Insulin, as a glucose uptake positive control, and Tomatidine, as a steroid-like negative control, were also tested.

Interestingly, not all Smo modulators induced noncanonical glucose uptake. Cyclopamine and GDC-0449 did, making them selective partial agonists, as did SAG and the two oxysterols—thus, dual agonists (Figures 7F, bottom, and S7B–S7D). Of these, all five elicited significant Ca^{2+} responses and muscle contractility (Figure 7F, top). Importantly, however, the reverse was not true. Not all Ca^{2+}-inducing modulators elicited a glucose uptake response (e.g., SANT-1, XL-139, and LDE-225). Thus, whereas Smo-ligand-induced glucose uptake appears to require Ca^{2+} induction, the processes can be pharmacologically uncoupled. Of note, SANT-1, XL-139, and LDE-225 all block the initial Smo translocation step to the cilium, suggesting additional support for the basal-body-dependent mechanism presented above and consistent with recently proposed multistep activation models of Smo action. Thus, whereas Ca^{2+} influx is required for the glucose uptake response, Smo-dependent Ca^{2+} induction alone does not induce metabolic rewiring.

Focusing on contractility, all Smo modulators with the exception of jervine induced Ca^{2+} influx in the nanomolar range (Figure 7F). Interestingly, not all canonical agonists induced glucose uptake. Despite significant Ca^{2+} and canonical activation signatures, purmorphamine showed no induction of noncanonical activity. Similarly, jervine showed no induction of any noncanonical response, Ca^{2+} or glucose. It will be of great interest to see how Smo "activation" by SAG, cyclopamine, jervine, and purmorphamine differ at the protein structure level. Together, these four compounds can independently uncouple canonical activation, canonical inhibition, Ca^{2+} signals, and Ampk signals—presumably all via the same receptor.

Perhaps most relevant to muscle side effects in humans, however, the finding that jervine exhibits canonical inhibition absent of both Ca^{2+} and glucose uptake responses predicts that development of small molecule inhibitors minimally impacting muscle contractility is possible. To gauge this hypothesis in vitro, we have now tested SAG, cyclopamine, GDC-0449, and jervine in primary human myocytes. Importantly, in keeping with the 3T3-L1 data, SAG, cyclopamine, and GDC-0449 all induced robust glucose uptake and P-AMPK responses (Figures 7H and S7E) in human muscle. They do so in the nanomolar range, and in keeping with our Ca^{2+} data, all three compounds elicit twitching of the human muscle fibers. Again and critically important, jervine showed no induction of glucose uptake, Ca^{2+}, or myocyte twitching. Thus, Smo-induced noncanonical glucose uptake and muscle contraction are conserved in primary human muscle cells.

Considering the implications for design of future hedgehog therapeutics for cancer and other diseases, a rigorous analysis of the Smo-induced contractile responses appears to be of immediate and paramount importance.

DISCUSSION

Here, we show that a Smo-dependent noncanonical signal rewires metabolism in vitro and in vivo. This Smo-Camkk2-Ampk axis can be uncoupled from the canonical pathway at the level of Smo, and cyclopamine and GDC-0449 are selective partial agonists of this rapid rewiring effect, whereby selective partial agonists are defined as compounds that are capable of differentially regulating two independent pathways via the same receptor. These demonstrations provide fundamental insights into Smo signaling, have substantial implications for ongoing Smo modulator development for cancer, and open the door for Smo-selective partial agonism as a new therapeutic strategy for obesity and diabetes.

We previously reported that mice with constitutively active canonical hedgehog signaling in adipose tissue exhibit a unique healthy phenotype despite striking white-adipose-specific lipoatrophy (Pospisilik et al., 2010). Those findings identified hedgehog signaling as one of the first hormonal axes capable of differentially regulating WAT and BAT adipogenesis. Interestingly, we once again observe BAT selectivity in the in vivo glucose uptake response to noncanonical agonism. What

distinguishes the responsive tissues (BAT/red muscle) from the less responsive ones (WAT/white muscle)? Systematic analysis across more than 25 mouse tissues showed no evidence for expression-based mechanism of either the canonical or noncanonical hedgehog arms. Several of our own unpublished observations, however, support the concept that metabolic profile might determine responsiveness, including a strong TZD dependence of the phenotype and metabolic epistasis that appears to favor glycolytic metabolic profiles (R.T., J.A.P., and H.E. unpublished data). Certainly critical for the lack of white adipose tissue responsiveness in vivo, AMPK actually reduces glucose uptake in this tissue, keeping with its primary role as a storage organ (Towler and Hardie, 2007).

Indeed, our data reveal a profound role for Smo signaling in regulating metabolic flux, specificity, and flexibility (Figure 7). These data are supported by our own transcriptional profiling of 3T3-L1 cells after 2 days of Shh stimulation that reveal highly significant enrichment scores for data sets associated with invasive cancer, hypoxia, and the transcriptional regulator Hif1α—signatures that clustered around downregulation of the KEGG/Biocarta pathways *oxidative phosphorylation*, *pyruvate metabolism*, and the *TCA cycle*, among others (J.A.P. and H.E., unpublished data). This finding indicates that canonical signaling reinforces the observed noncanonical metabolic routing by initiating a transcriptional aerobic glycolysis response and modulating expression of the entire machinery of primary metabolism.

Transcriptional reinforcement aside, however, we see Smo-selective partial agonism doubling whole-body glucose uptake within ~30 min. Also, we observe an apparent parallel activation of thermogenesis with similar kinetics. The data therefore raise Smo-selective partial agonism as a therapeutic option for obesity and types-1 and -2 diabetes. But more fundamentally, they demonstrate a dominant physiological response of noncanonical hedgehog signaling in vivo. What additional noncanonical responses exist physiologically? Do endogenous ligands exist that selectively activate either canonical or noncanonical signaling? Certainly the two oxysterols 20(s)OHC and 25OHC are capable. To what extent do these factors underlie previous "canonical" effects? All of these questions are open.

Many molecules have been shown to stimulate Smo-dependent signaling (Chen et al., 2002b; Corcoran and Scott, 2006; Nachtergaele et al., 2012; Sinha and Chen, 2006; Wang et al., 2010). Although screening efforts typically rely on canonical readouts such as Gli-responsive luciferase reporters, few have interrogated noncanonical signaling in parallel. Systematic characterization of selective partial agonism should provide insights into the biochemical requirements that are necessary for canonical versus noncanonical stimulation and structural rationale for design of Smo-selective partial agonists. Based on what we know, such Smo modulators, much like the very pleiotropic selective estrogen receptor modulators (SERMs) (Riggs and Hartmann, 2003), should have the potential to impact multiple Ampk-dependent pathways in and beyond metabolism, including cell size (kidney) and immune cell polarity (macrophages).

The uncoupling of canonical/noncanonical signals and activation of the Smo-Ampk axis by both SAG and cyclopamine represent a paradigm shift. The findings add a new level of complexity with which a cell can establish downstream signaling diversity and cell type specificity. Cyclopamine has been shown to inhibit some noncanonical signals (Chinchilla et al., 2010; Polizio et al., 2011; Riobo et al., 2006). What distinguishes our findings from those? First, kinetics. Previous reports have used long-term measures to assess their effects. Perhaps more likely, however, is the second messenger system in question and subcellular localization, for instance, at the cilium.

The last decade of hedgehog research has seen substantial advances toward unraveling a "Gli code" and linking ligand binding to transcriptional output (Hui and Angers, 2011; Ruiz i Altaba et al., 2007). That said, a number of deep-seated paradigms remain enigmatic: the nature of Gli target specification, Gli target gene set expansion with signal intensity, and the inconsistencies in potency of pathway inhibition versus potency of cancer growth inhibition. The demonstrations that hedgehog rewires metabolism and that canonical and noncanonical paths are independent reveal functional plasticity that may—at least in part—explain these notions. For instance, metabolic state alone can drive dramatic cell fate transitions and expression changes (e.g., immune cell polarity, activation state, cancer invasiveness, etc.) (Hitosugi et al., 2009; Hsu and Sabatini, 2008; Jeon et al., 2012; Shi et al., 2011). Indeed, it will be intriguing to see to what extent hedgehog's multiple procancer effects depend on acute or chronic changes in metabolic state. We feel that, to properly understand hedgehog phenotype, future analyses must include secondary messenger repertoire of the system in question and its respective noncanonical outputs.

Along similar lines, if canonical and noncanonical arms are independent, then as long as Smo is expressed, the potential for a noncanonical response remains. GPCRs have the potential to signal when internalized (Calebiro et al., 2010); some even change their downstream effectors accordingly. Oxysterol binding to Smo has recently been shown to allosterically amplify hedgehog output (Corcoran and Scott, 2006; Nachtergaele et al., 2012). We now show that they activate metabolic rewiring. These cell-permeable lipid derivatives are quantitatively dynamic and found throughout the cell, and they respond to the metabolic milieu. Should the notion of hedgehog responsiveness be fine-tuned? Are some hedgehog nonresponsive cell types still competent for noncanonical signals and metabolic rewiring? These questions too are now open.

EXPERIMENTAL PROCEDURES

Cell Culture

Primary brown preadipocytes, MEFs, C2C12s, and mouse 3T3-L1 preadipocytes (ATCC) were grown and differentiated as described (Pospisilik et al., 2010; Todoric et al., 2011; Varjosalo et al., 2006; Wong et al., 2009). Before stimulations, cells were starved overnight in DMEM containing 1% BSA. All stimulations were performed in starvation medium. Human myoblast cultures and myocytes were established from four human study subjects according to Gaster et al. (2002).

Cellular O_2/CO_2 Exchange

A Seahorse XF24 Extracellular Flux Analyzer (Seahorse Bioscience) was used to analyze bioenergetic function of cells. Cellular DNA was measured to adjust for potential differences in cell densities.

Metabolites

NAD^+, $NADP^+$, NADH, NADPH, glucose, and lactate were determined using commercially available kits (Bioassay Systems). AMP, ADP, and ATP were determined as described (Liu et al., 2010).

shRNA

Lentiviruses expressing targeting shRNAs were used to transduce cells according to standard protocols. Puromycin was used to select stable clones.

Phospho-Protein Enrichment, 2D-PAGE, and Mass Spectrometry

Phosphoproteins of total adipocyte protein were enriched by affinity column purification, isoelectric focused, and separated by SDS-PAGE. Detection, matching, background subtraction, normalization, and quantitative comparison of scanned 2D spots used Progenesis SameSpots software (Nonlinear Dynamics). Spots were excised, tryptic digested, identified, and quantified using an XCT-Ultra mass spectrometer.

AMPKAR-Foerster Resonance Energy Transfer Assay

Real-time AMPK activation was recorded using the AMPKAR-FRET construct as described (Tsou et al., 2011).

Ca^{2+} Signal Measurements

FluoForte AM (Enzo Lifescience) was used to measure dynamic changes of intracellular calcium levels according to the manufacturer's instructions.

Glucose Uptake

Basal glucose uptake of human myotubes was determined by capturing 2-[1-^{14}C]-deoxy-glucose (Perkin Elmer) as previously described (Gaster et al., 2002).

Quantitative RT-PCR Analysis

Total RNA was extracted using TRIzol. cDNA was prepared with the iScript cDNA Synthesis Kit (Bio-Rad). qPCR was run using intron-spanning and junction primer pairs on an AbiPRISM 7500fast real-time cycler (Applied Biosystems) using the iQ SYBR Green Supermix (Bio-Rad).

Phenotype Microarrays

Phenotype microarray experiments were performed following protocols provided by Biolog Inc. (http://www.biolog.com/).

Animal Experiments

Eight- to 11-week-old, overnight fasted C57BL/6J male mice were used for in vivo studies. For cyclopamine testing, mice were injected intraperitoneally (i.p.) with vehicle (45% HBS) or cyclopamine (10 mg/kg) either alone or in conjunction with a 1 g/kg OGTT. STZ induction was i.p. (200 mg/kg) followed by a 72 hr stabilization period. For clamps, femoral catheterized mice were infused continuously with 1 μg/kg/min somatostatin, and glycemia was clamped to 12.5 mM by variable infusion of 10% glucose. Mice were maintained at steady state for 90 min prior to cyclopamine administration.

Statistical Analysis

Data sets were compared for statistical significance using a two-tailed Student's t test, and data are expressed as mean ± SEM unless otherwise specified. $p < 0.05$ was considered significant.

SUPPLEMENTAL INFORMATION

Supplemental information includes Extended Experimental Procedures, seven figures, and two tables and can be found with this article online at http://dx.doi.org/10.1016/j.cell.2012.09.021.

ACKNOWLEDGMENTS

The authors are indebted to the DART, AIRC, Marie-Curie, and JDRF for fellowships and WWTF, MPG, FWF, FFG (GenAU-program), and OeAW for funding. S.L.M. is a Career Development Fellow and M.A.F. a Senior Research Fellow of the National Health and Medical Research Council of Australia. The authors are grateful to E. Hobeika, M. Bilban, E. Einwallner, A. Jais, I. Lynfort, and B. Vind for critical technical and theoretical help. The authors are also grateful to M. Scott for providing Smoothened expression constructs, to J. Reiter for Smo-CLD and providing *Kif3a*$^{-/-}$ and *Ift88*$^{-/-}$ cells, to J. Taipale for providing *Smo*$^{-/-}$ cells, and to L. Cantley for the AMPKAR vector.

Received: February 28, 2012
Revised: June 18, 2012
Accepted: September 17, 2012
Published: October 11, 2012

REFERENCES

Belgacem, Y.H., and Borodinsky, L.N. (2011). Sonic hedgehog signaling is decoded by calcium spike activity in the developing spinal cord. Proc. Natl. Acad. Sci. USA *108*, 4482–4487.

Boehlke, C., Kotsis, F., Patel, V., Braeg, S., Voelker, H., Bredt, S., Beyer, T., Janusch, H., Hamann, C., Gödel, M., et al. (2010). Primary cilia regulate mTORC1 activity and cell size through Lkb1. Nat. Cell Biol. *12*, 1115–1122.

Calebiro, D., Nikolaev, V.O., Persani, L., and Lohse, M.J. (2010). Signaling by internalized G-protein-coupled receptors. Trends Pharmacol. Sci. *31*, 221–228.

Cantó, C., and Auwerx, J. (2011). Calorie restriction: is AMPK a key sensor and effector? Physiology (Bethesda) *26*, 214–224.

Chen, J.K., Taipale, J., Cooper, M.K., and Beachy, P.A. (2002a). Inhibition of Hedgehog signaling by direct binding of cyclopamine to Smoothened. Genes Dev. *16*, 2743–2748.

Chen, J.K., Taipale, J., Young, K.E., Maiti, T., and Beachy, P.A. (2002b). Small molecule modulation of Smoothened activity. Proc. Natl. Acad. Sci. USA *99*, 14071–14076.

Chen, W., Tang, T., Eastham-Anderson, J., Dunlap, D., Alicke, B., Nannini, M., Gould, S., Yauch, R., Modrusan, Z., DuPree, K.J., et al. (2011). Canonical hedgehog signaling augments tumor angiogenesis by induction of VEGF-A in stromal perivascular cells. Proc. Natl. Acad. Sci. USA *108*, 9589–9594.

Chinchilla, P., Xiao, L., Kazanietz, M.G., and Riobo, N.A. (2010). Hedgehog proteins activate pro-angiogenic responses in endothelial cells through non-canonical signaling pathways. Cell Cycle *9*, 570–579.

Corbit, K.C., Aanstad, P., Singla, V., Norman, A.R., Stainier, D.Y., and Reiter, J.F. (2005). Vertebrate Smoothened functions at the primary cilium. Nature *437*, 1018–1021.

Corcoran, R.B., and Scott, M.P. (2006). Oxysterols stimulate Sonic hedgehog signal transduction and proliferation of medulloblastoma cells. Proc. Natl. Acad. Sci. USA *103*, 8408–8413.

Gaster, M., Petersen, I., Højlund, K., Poulsen, P., and Beck-Nielsen, H. (2002). The diabetic phenotype is conserved in myotubes established from diabetic subjects: evidence for primary defects in glucose transport and glycogen synthase activity. Diabetes *51*, 921–927.

Han, Y.G., Spassky, N., Romaguera-Ros, M., Garcia-Verdugo, J.M., Aguilar, A., Schneider-Maunoury, S., and Alvarez-Buylla, A. (2008). Hedgehog signaling and primary cilia are required for the formation of adult neural stem cells. Nat. Neurosci. *11*, 277–284.

Hardie, D.G. (2011). AMP-activated protein kinase: an energy sensor that regulates all aspects of cell function. Genes Dev. *25*, 1895–1908.

Hitosugi, T., Kang, S., Vander Heiden, M.G., Chung, T.W., Elf, S., Lythgoe, K., Dong, S., Lonial, S., Wang, X., Chen, G.Z., et al. (2009). Tyrosine phosphorylation inhibits PKM2 to promote the Warburg effect and tumor growth. Sci. Signal. *2*, ra73.

Hsu, P.P., and Sabatini, D.M. (2008). Cancer cell metabolism: Warburg and beyond. Cell *134*, 703–707.

Hui, C.C., and Angers, S. (2011). Gli proteins in development and disease. Annu. Rev. Cell Dev. Biol. *27*, 513–537.

Ingham, P.W., Nakano, Y., and Seger, C. (2011). Mechanisms and functions of Hedgehog signalling across the metazoa. Nat. Rev. Genet. *12*, 393–406.

Jeon, S.-M., Chandel, N.S., and Hay, N. (2012). AMPK regulates NADPH homeostasis to promote tumour cell survival during energy stress. Nature *485*, 661–665.

Li, Y., Maitah, M.Y., Ahmad, A., Kong, D., Bao, B., and Sarkar, F.H. (2012). Targeting the Hedgehog signaling pathway for cancer therapy. Expert Opin. Ther. Targets *16*, 49–66.

Lin, T.L., and Matsui, W. (2012). Hedgehog pathway as a drug target: Smoothened inhibitors in development. Onco. Targets Ther. *5*, 47–58.

Liu, Q., Gauthier, M.S., Sun, L., Ruderman, N., and Lodish, H. (2010). Activation of AMP-activated protein kinase signaling pathway by adiponectin and insulin in mouse adipocytes: requirement of acyl-CoA synthetases FATP1 and Acsl1 and association with an elevation in AMP/ATP ratio. FASEB J. *24*, 4229–4239.

Low, J.A., and de Sauvage, F.J. (2010). Clinical experience with Hedgehog pathway inhibitors. J. Clin. Oncol. *28*, 5321–5326.

Lowe, C.E., O'Rahilly, S., and Rochford, J.J. (2011). Adipogenesis at a glance. J. Cell Sci. *124*, 2681–2686.

Lumeng, C.N., and Saltiel, A.R. (2011). Inflammatory links between obesity and metabolic disease. J. Clin. Invest. *121*, 2111–2117.

Nachtergaele, S., Mydock, L.K., Krishnan, K., Rammohan, J., Schlesinger, P.H., Covey, D.F., and Rohatgi, R. (2012). Oxysterols are allosteric activators of the oncoprotein Smoothened. Nat. Chem. Biol. *8*, 211–220.

Ng, J.M.Y., and Curran, T. (2011). The Hedgehog's tale: developing strategies for targeting cancer. Nat. Rev. Cancer *11*, 493–501.

Nüsslein-Volhard, C., and Wieschaus, E. (1980). Mutations affecting segment number and polarity in Drosophila. Nature *287*, 795–801.

Ogden, S.K., Fei, D.L., Schilling, N.S., Ahmed, Y.F., Hwa, J., and Robbins, D.J. (2008). G protein Galphai functions immediately downstream of Smoothened in Hedgehog signalling. Nature *456*, 967–970.

Polizio, A.H., Chinchilla, P., Chen, X., Kim, S., Manning, D.R., and Riobo, N.A. (2011). Heterotrimeric Gi proteins link Hedgehog signaling to activation of Rho small GTPases to promote fibroblast migration. J. Biol. Chem. *286*, 19589–19596.

Pospisilik, J.A., Schramek, D., Schnidar, H., Cronin, S.J.F., Nehme, N.T., Zhang, X., Knauf, C., Cani, P.D., Aumayr, K., Todoric, J., et al. (2010). Drosophila genome-wide obesity screen reveals hedgehog as a determinant of brown versus white adipose cell fate. Cell *140*, 148–160.

Riggs, B.L., and Hartmann, L.C. (2003). Selective estrogen-receptor modulators — mechanisms of action and application to clinical practice. N. Engl. J. Med. *348*, 618–629.

Riobo, N.A., and Manning, D.R. (2007). Pathways of signal transduction employed by vertebrate Hedgehogs. Biochem. J. *403*, 369–379.

Riobo, N.A., Saucy, B., Dilizio, C., and Manning, D.R. (2006). Activation of heterotrimeric G proteins by Smoothened. Proc. Natl. Acad. Sci. USA *103*, 12607–12612.

Rohatgi, R., and Scott, M.P. (2007). Patching the gaps in Hedgehog signalling. Nat. Cell Biol. *9*, 1005–1009.

Rohatgi, R., Milenkovic, L., and Scott, M.P. (2007). Patched1 regulates hedgehog signaling at the primary cilium. Science *317*, 372–376.

Rohatgi, R., Milenkovic, L., Corcoran, R.B., and Scott, M.P. (2009). Hedgehog signal transduction by Smoothened: pharmacologic evidence for a 2-step activation process. Proc. Natl. Acad. Sci. USA *106*, 3196–3201.

Roudaut, H., Traiffort, E., Gorojankina, T., Vincent, L., Faure, H., Schoenfelder, A., Mann, A., Manetti, F., Solinas, A., Taddei, M., and Ruat, M. (2011). Identification and mechanism of action of the acylguanidine MRT-83, a novel potent Smoothened antagonist. Mol. Pharmacol. *79*, 453–460.

Ruiz i Altaba, A., Mas, C., and Stecca, B. (2007). The Gli code: an information nexus regulating cell fate, stemness and cancer. Trends Cell Biol. *17*, 438–447.

Sekulic, A., Migden, M.R., Oro, A.E., Dirix, L., Lewis, K.D., Hainsworth, J.D., Solomon, J.A., Yoo, S., Arron, S.T., Friedlander, P.A., et al. (2012). Efficacy and safety of vismodegib in advanced basal-cell carcinoma. N. Engl. J. Med. *366*, 2171–2179.

Shi, L.Z., Wang, R., Huang, G., Vogel, P., Neale, G., Green, D.R., and Chi, H. (2011). HIF1alpha-dependent glycolytic pathway orchestrates a metabolic checkpoint for the differentiation of TH17 and Treg cells. J. Exp. Med. *208*, 1367–1376.

Sinha, S., and Chen, J.K. (2006). Purmorphamine activates the Hedgehog pathway by targeting Smoothened. Nat. Chem. Biol. *2*, 29–30.

Suh, J.M., Gao, X., McKay, J., McKay, R., Salo, Z., and Graff, J.M. (2006). Hedgehog signaling plays a conserved role in inhibiting fat formation. Cell Metab. *3*, 25–34.

Tang, J.Y., Mackay-Wiggan, J.M., Aszterbaum, M., Yauch, R.L., Lindgren, J., Chang, K., Coppola, C., Chanana, A.M., Marji, J., Bickers, D.R., and Epstein, E.H., Jr. (2012). Inhibiting the hedgehog pathway in patients with the basal-cell nevus syndrome. N. Engl. J. Med. *366*, 2180–2188.

Teglund, S., and Toftgård, R. (2010). Hedgehog beyond medulloblastoma and basal cell carcinoma. Biochim. Biophys. Acta *1805*, 181–208.

Theunissen, J.W., and de Sauvage, F.J. (2009). Paracrine Hedgehog signaling in cancer. Cancer Res. *69*, 6007–6010.

Todoric, J., Strobl, B., Jais, A., Boucheron, N., Bayer, M., Amann, S., Lindroos, J., Teperino, R., Prager, G., Bilban, M., et al. (2011). Cross-talk between interferon-γ and hedgehog signaling regulates adipogenesis. Diabetes *60*, 1668–1676.

Towler, M.C., and Hardie, D.G. (2007). AMP-activated protein kinase in metabolic control and insulin signaling. Circ. Res. *100*, 328–341.

Tsou, P., Zheng, B., Hsu, C.-H., Sasaki, A.T., and Cantley, L.C. (2011). A fluorescent reporter of AMPK activity and cellular energy stress. Cell Metab. *13*, 476–486.

Vander Heiden, M.G., Cantley, L.C., and Thompson, C.B. (2009). Understanding the Warburg effect: the metabolic requirements of cell proliferation. Science *324*, 1029–1033.

Varjosalo, M., Li, S.-P., and Taipale, J. (2006). Divergence of hedgehog signal transduction mechanism between Drosophila and mammals. Dev. Cell *10*, 177–186.

Von Hoff, D.D., LoRusso, P.M., Rudin, C.M., Reddy, J.C., Yauch, R.L., Tibes, R., Weiss, G.J., Borad, M.J., Hann, C.L., Brahmer, J.R., et al. (2009). Inhibition of the hedgehog pathway in advanced basal-cell carcinoma. N. Engl. J. Med. *361*, 1164–1172.

Wang, Y., Zhou, Z., Walsh, C.T., and McMahon, A.P. (2009). Selective translocation of intracellular Smoothened to the primary cilium in response to Hedgehog pathway modulation. Proc. Natl. Acad. Sci. USA *106*, 2623–2628.

Wang, J., Lu, J., Bond, M.C., Chen, M., Ren, X.R., Lyerly, H.K., Barak, L.S., and Chen, W. (2010). Identification of select glucocorticoids as Smoothened agonists: potential utility for regenerative medicine. Proc. Natl. Acad. Sci. USA *107*, 9323–9328.

Whittle, A.J., López, M., and Vidal-Puig, A. (2011). Using brown adipose tissue to treat obesity - the central issue. Trends Mol. Med. *17*, 405–411.

Wong, S.Y., Seol, A.D., So, P.L., Ermilov, A.N., Bichakjian, C.K., Epstein, E.H., Jr., Dlugosz, A.A., and Reiter, J.F. (2009). Primary cilia can both mediate and suppress Hedgehog pathway-dependent tumorigenesis. Nat. Med. *15*, 1055–1061.

Yam, P.T., Langlois, S.D., Morin, S., and Charron, F. (2009). Sonic hedgehog guides axons through a noncanonical, Src-family-kinase-dependent signaling pathway. Neuron *62*, 349–362.

Yauch, R.L., Gould, S.E., Scales, S.J., Tang, T., Tian, H., Ahn, C.P., Marshall, D., Fu, L., Januario, T., Kallop, D., et al. (2008). A paracrine requirement for hedgehog signalling in cancer. Nature *455*, 406–410.